Dynamic properties and the two-point correlation function for electrons in localized coherent Langmuir fields

Cangtao Zhou, Shao-ping Zhu, and X. T. He
Center for Nonlinear Studies, Institute of Applied Physics and Computational Mathematics, P.O. Box 8009, Beijing 100088, China
(Received 12 September 1991; revised manuscript received 30 March 1992)

The dynamic properties for electrons in the localized coherent Langmuir wave fields have been investigated numerically. The Poincaré map and the absolute diffusion coefficient account for the existence of regular islands embedded within stochastic regions of phase space. The relative diffusion behavior illustrates that the localized coherent Langmuir wave packets can lead to the formation of a microscale correlation for electrons in phase space. The time evolution of relative quantities further shows that such a microscale correlation has the characteristic of phase-space particle-density granulations, although the electric fields are regular. Finally, the two-point correlation function has been measured by use of the particle simulation technique. That the strong peak behavior of the correlation function can occur only for sufficiently small r^0 and u^0 has been displayed by the simulated results. All these phenomena indicate that the microscale correlation effects (defined also as "clumps") indeed exist in our dynamic system.

PACS number(s): 52.35.Mw, 52.65.+z, 05.45.+b

I. INTRODUCTION

An important subject in nonlinear plasma physics is the study of the dynamic properties of particles due to the acceleration of charged particles by localized coherent Langmuir wave packets. In a previous paper [1] we have obtained a relative diffusion coefficient for electrons interacting with coherent wave fields. It is revealed that the coherent fields can derive the formation of the microscale correlation. The lifetime of the microscale correlation diverges logarithmically when the relative positions become closer.

On the other hand, many results had also been obtained in the study of acceleration of electrons by localized fields. Fuchs *et al.* [2] used a quasilinear diffusion model to describe particles interacting periodically with coherent wave packets. Colunga, Luciani, and Mora [3] studied the acceleration of electrons by the fields produced during resonance absorption of laser light. Rozmus and co-workers [4,5] and one of the present authors [6] discussed the particle dynamics. Their theoretical model for the absolute diffusion coefficient accounts for the existence of large adiabatic islands, embedded within the stochastic region of the phase space.

In turbulence plasma, a very important phenomenon, clumps, in which particles are granulated by random electric fields, has been investigated extensively [7–13]. Dupree [8] has pointed out that the microscale random phase-space granulations or clumps arise because the Vlasov equation preserves phase-space density along particle orbits. The densities at neighboring phase-space points may originally have been widely separated in phase space. The granulations are due to the mixing of "fluids" of different densities that do not interpenetrate owing to Liouville's theorem.

In Ref. [1], we reported that the coherent Langmuir wave fields may lead to the microscale correlation, where the characteristic is similar to that of clump effects, and defined this microscale correlation as "clumps." The main purpose in this paper is to study the dynamic properties of electrons interacting with the localized coherent Langmuir wave packets, systematically. In particular, we want to know whether the features of clumps discussed by Dupree and others can indeed be exhibited in our dynamics systems, even where the electric fields interacting with electrons are regular.

In Sec. II the theoretical model is discussed. The absolute diffusion, the relative diffusion, etc., dynamic properties, have been discussed in Secs. III and IV, respectively. In Sec. V the two-point correlation function has been measured by the particle simulation technique. Finally some conclusions are given in Sec. VI.

II. DESCRIPTION OF LOCALIZED COHERENT LANGMUIR WAVE PACKETS

The coupled nonlinear equations, known as Zakharov equations [14], describe the nonlinear interaction between a high-frequency Langmuir wave and a low-frequency ion acoustic wave by the ponderomotive force. Under the subsonic regime, Zakharov equations can be reduced to the cubically nonlinear Schrödinger equation. The electric field $E(X,t)$ that may be obtained from a stationary solution of the Zakharov equations or the cubically nonlinear Schrödinger one can be expressed in the following form:

$$E(X,t)=E_0\mathrm{sech}(gX)\cos(\omega_p t)\ , \tag{1}$$

where

$$g=\frac{1}{\sqrt{3}\lambda_D}\frac{E_0}{\sqrt{8\pi n_e k_B T}},$$

$$\lambda_D=\left[\frac{k_B T}{4\pi e^2 n_e}\right]^{1/2},$$

$$\omega_p=\left[\frac{4\pi e^2 n_e}{m_e}\right]^{1/2},$$

E_0 is the amplitude, T the electron temperature, n_e the electron number density, and m_e the electron mass.

Consider a model for describing electrons interacting with the localized coherent Langmuir wave packets, as discussed by Rozmus and co-workers [4,5]. The wave packets in each structure are of the form of expression (1). Extending sech(gx) with a periodic length L, we have the equations of motion for the test particles in the dimensionless form

$$\frac{dX_i(t)}{dt}=V_i,$$
$$\frac{dV_i(t)}{dt}=-\sum_{n=-N}^{N}E_n\cos[K_n X_i(t)-t], \tag{2}$$

where $K_n=2\pi n/L$, E_n is in units of $\sqrt{8\pi n_e k_B T}$, and space and time are in the Debye length λ_D and $1/\omega_p$, respectively. In the following numerical discussions, we choose parameters $E_0^2/8\pi n_e k_B T=0.4$, $L=32$. In order to exhibit the characteristic of the soliton envelope (1) in each periodic structure in terms of the Fourier modes E_n, we truncate the summation in Eq. (2) as $E_{\pm N}/E_0\sim(10^{-3})$. The soliton structure and the spectrum of the wave packets are presented in Fig. 1.

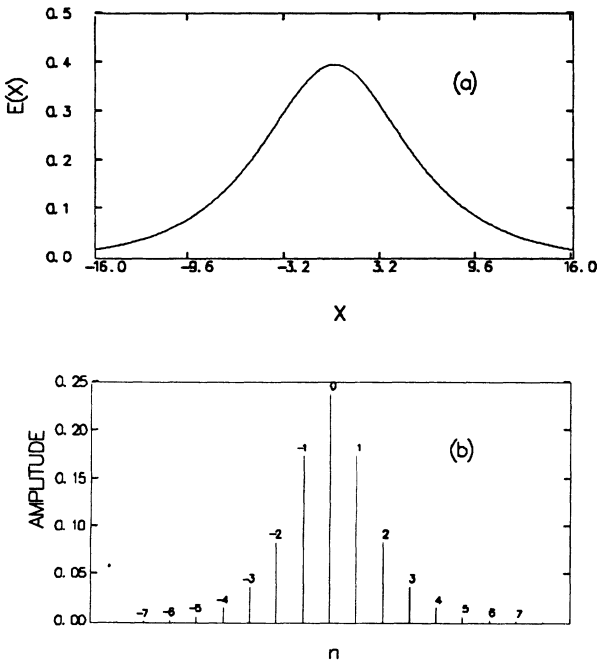

FIG. 1. (a) Soliton envelope. (b) Spectrum of the wave packet.

III. ABSOLUTE DIFFUSION

The numerical solution of Eq. (2) is depicted in the phase-space plots in Fig. 2(a), which is produced by mapping the particles velocities and positions at intervals of $T_p=2\pi$. Figure 2(a) clearly illustrates that the stochastic regions are not uniformly filled with the phase space. Several areas with the trapped orbits, characterized by regular trajectories, exist within the stochastic region.

According to the resonant overlapping criterion [15,16],

$$\tfrac{1}{2}(\Delta V_n+\Delta V_{n+1})>\left|\frac{\omega_p}{K_n}-\frac{\omega_p}{K_{n+1}}\right|, \tag{3}$$

where $\Delta V_n=4(E_n/K_n)^{1/2}$ corresponds to the width of the unperturbed trapping region of the nth mode. We find that all modes except $n=0$ satisfy the overlapping criterion. The trapping regions of the $n=0$ mode are separated from the stochastic bands by intervals with regular untrapped orbits. The regular islands embedded in the stochastic regions are the first-order resonances related to the overlapping criterion [17]. The influence of the high-order resonances can also be observed in Fig. 2(a). Thus the irregular motion, trapped orbits, secondary resonance, and the Kolmogorov-Arnold-Moser (KAM) surfaces must simultaneously be considered. The chaotic motion of electrons arises from the coherent Langmuir wave packets. The absolute diffusion of the random particles can be measured as follows:

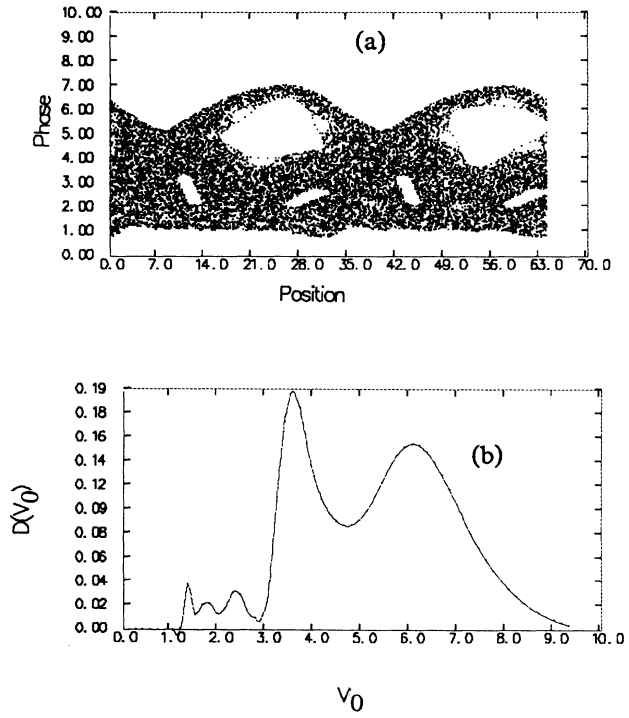

FIG. 2. (a) Poincaré surface of the section plot, based on numerical solutions to the equations of motions (2). (b) Absolute diffusion coefficient.

$$D(V_0)=\frac{1}{2\tau_d}\langle[V(t)-V_0]^2\rangle\ , \tag{4}$$

where $\tau_d=L/V_0$ is the approximated time for one pass through the periodic structures, and the symbol $\langle\ \rangle$ denotes an ensemble average. The ensemble average in all the numerical discussions is computed by averaging over a set of particles with different start times but with the same initial velocities and positions.

Figure 2(b) shows the numerical results for the absolute diffusion coefficient calculated from Eq. (4). The stable islands in the stochastic region [see Fig. 2(a)] have also been displayed in Fig. 2(b). When the particle's velocities are close to zero, particles experience a ponderomotive potential and are trapped by this potential well. The diffusion coefficient near zero velocity is zero. The diffusion increases in the stochastic region and decreases near the stable islands. With the increase of the initial velocity (which depends on the energy in the system), the separation layer forms in phase space and the diffusion coefficient also tends to zero.

IV. RELATIVE DIFFUSION PROPERTIES

The absolute diffusion coefficient only displays the dynamic behavior of one particle in phase space. To describe the features of the neighbor particles, we introduce the relative and barycentric motion coordinates

$$r=X_1-X_2\ ,\quad R=X_1+X_2\ , \tag{5}$$
$$u=V_1-V_2\ ,\quad U=V_1+V_2\ .$$

The equations of the relative motions become

$$\frac{dr}{dt}=u\ ,\quad \frac{du}{dt}=\sum_n 2E_n\sin\left[\frac{K_nR}{2}-t\right]\sin\left[\frac{K_nr}{2}\right]\ , \tag{6}$$
$$\frac{dR}{dt}=U\ ,\quad \frac{dU}{dt}=-\sum_n 2E_n\cos\left[\frac{K_nR}{2}-t\right]\cos\left[\frac{K_nr}{2}\right]\ .$$

First, we discuss the relative diffusion behaviors and define the relative diffusion coefficient as

$$D^u_-(R,r,U,u)=\frac{1}{2\tau_d}\langle[u(t)-u^0]^2\rangle \tag{7}$$

for the velocity space, and

$$D^r_-(R,r,U,u)=\frac{1}{2\tau_d}\langle[r(t)-r^0]^2\rangle \tag{8}$$

for the configuration space, where $\tau_d=\frac{1}{2}(L/V_1^0+L/V_2^0)$. In the previous study [1], we only considered the relative diffusion in velocity space; here, we also do the relative diffusion in configuration space. From Figs. 3 and 4 we see that D^i_-. $(i=u,r)$ decreases for small r^0 with decreasing u^0. In other words, it shows that the relative diffusion slows down considerably when the relative motion trajectories become closer and closer. These numerical results for the relative diffusion coefficient indicate the existence of the microscale correlation. The fact that D^i_- has a nonzero minimum means that the lifetime

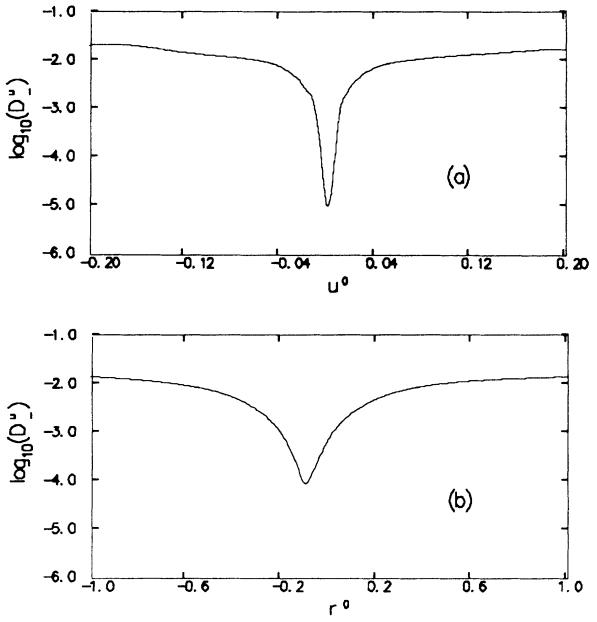

FIG. 3. Relative diffusion coefficient in velocity space. (a) Relative diffusion coefficient vs the relative velocities when $r^0=0.01$. (b) Relative diffusion coefficient vs the relative coordinates with $u^0=0.01$.

is finite. The lifetime τ_{cl} (also called clump lifetime) may be obtained from [8–10]

$$K_c^2\langle r^2(\tau_{cl})\rangle=1\ , \tag{9}$$

where K_c is the characteristic wave number. For our dy-

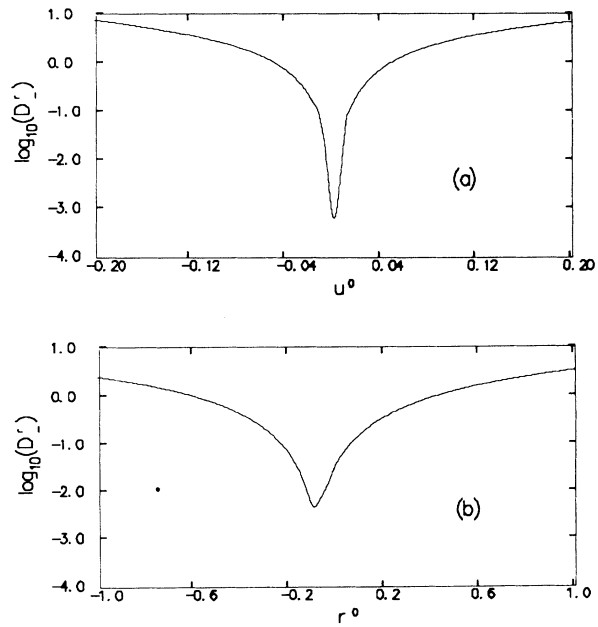

FIG. 4. Relative diffusion coefficient in configuration space. (a) Relative diffusion coefficient vs the relative velocities with $r^0=0.01$. (b) Relative coefficient vs the relative coordinates with $u^0=0.01$.

namic system we have [1]

$$\tau_{\rm cl}=a-b\ln r^0 , \tag{10}$$

where a,b are positive constants. We find that $\tau_{\rm cl}$ diverges logarithmically as r^0 vanishes, and is much greater than the coherent time [1]

$$\tau_c=\left[\frac{2}{K_c^2(D_1+D_2)}\right]^{1/3} , \tag{11}$$

where D_1 and D_2 are the absolute diffusion coefficients for two neighboring particles.

The lifetime may also be analyzed in terms of the time evolutions of the relative quantities. In the stochastic regime, the neighboring particles are of the exponential separation type [17]. For plasma turbulence, Dupree [7–9] showed that the exponential separation trajectories occur over most of the clump scale. Misguich and Balescu [18] even illustrated that the relative diffusion of charged particles in turbulent electric fields can be divided into three time regions, i.e., a short-time regime (of order τ_c), a trajectory renormalization regime, and a long-time regime. The clump behavior is associated with the trajectory renormalization regime. In the second region, there exists a universal behavior for the relative evolution, that is,

$$\langle r^2(t)\rangle \sim e^{t/\tau_0} , \tag{12}$$

where τ_0 corresponds to the diffusion time scale. They pointed out that this exponential behavior is due to an extrinsic turbulence field [18]. This extrinsic stochasticity leads to a finite clump lifetime.

In Fig. 5(a), we give the time evolution of the neighboring particles. Obviously, the exponential separation also exists in our dynamic system, where chaotic behavior results from an intrinsic stochasticity. The evolution of the separation of neighboring trajectories permits a determination of the lifetime of microscale correlation. From Fig. 5(a), we observe that $\ln\langle r^2(t)\rangle \sim t$ as $t<70$. On the other hand, Fig. 5(b) indicates that the relative velocity of neighboring particles basically remains invariable as $t<70$. In a sense, the neighboring particles in sufficiently small phase-space cells suffer the same force, which is just the property of clumps.

Another characteristic quantity that can account for the clump effects is $K_\xi=\langle\xi^4\rangle/\langle\xi^2\rangle^2$. When a random quantity $\xi(t)$ is a Gaussian process, the magnitude of the fourth cumulant $\langle\xi^4\rangle-3\langle\xi^2\rangle^2$ vanishes. The kurtosis of K_ξ is associated with the clump lifetime [19]. Pettini *et al.* pointed out that the clump time scale (at which the peaks of K_ξ occur) can be related to the Kolmogorov-Sinai (KS) entropy. Figure 6 clearly displays a strong peak behavior around the lifetime of microscale correlation. With the evolution of time, K_r tends to a constant.

Now, we simply summarize our numerical results and give a basically physical picture. For homogeneous or weak inhomogeneous plasma, the stochastic electric fields leads to the chaotic diffusion of particles. When regions of different phase-space density are mixed by the fluctuating electric fields or magnetic fields, the microscale random phase-space granulations or clumps are produced [7–13]. For our dynamic system, the particle stochasticity arises from the localized coherent Langmuir wave packets, where the phase velocities of the modes satisfy the overlapping criterion. The numerical results show that the microscale correlation also exists in our dynamic system. Now we can conclude that such a microscale correlation has indeed the characteristic of clumps. In order to illustrate this feature, we further investigate the statistical behavior, where the two-point correlation function will be measured by the particle simulation technique.

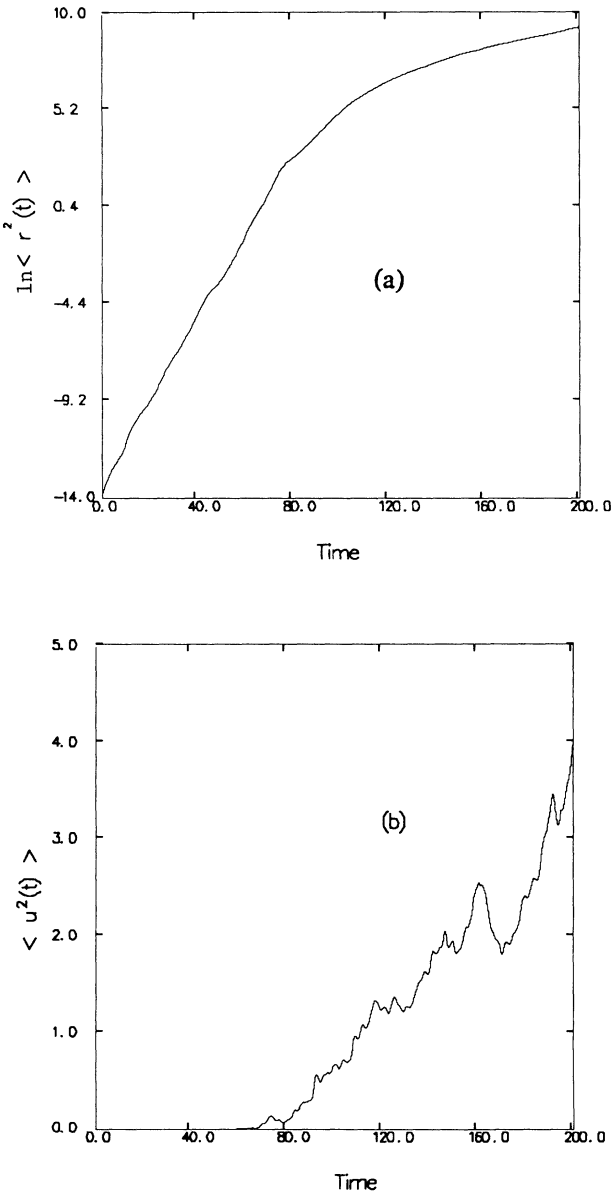

FIG. 5. (a) Time evolution of $\langle r^2(t)\rangle$. (b) Time evolution of $\langle u^2(t)\rangle$. The parameter values correspond to $r^0=0.001$ and $u^0=0.0002$.

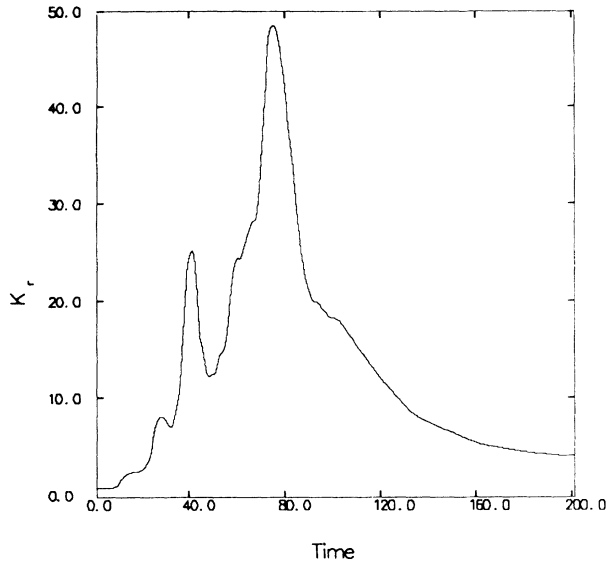

FIG. 6. Time evolution of K_r, where the kurtosis is associated with the lifetime of the microscale correlation.

V. TWO-POINT CORRELATION FUNCTION

To finish the particle simulation, we must choose an initial background distribution function. In the work discussed by Hui and Dupree, they only involved the spatial homogeneous or weak inhomogeneous plasmas. Thus an initial Maxwellian distribution was considered. For our system, the initial Maxwellian distribution is obviously not available due to the existence of spatial structure for electric fields.

In nonlinear plasma theory, the fact is that the soliton fields developed by modulational instability can well be explained in terms of Zakharov equations or the cubically nonlinear Schrödinger equation. However, the particle distribution function trapped by wave fields cannot be given by these equations. On the other hand, if we divide the Vlasov distribution function into three parts: δf, δF, and F_0, where δf is a fast varying fluctuation and corresponds to a high-frequency (HF) oscillation, and δF is a slowly varying coherent part and corresponds to a low-frequency (LF) oscillation. Also, the electric fields should include the HF field E_f and the LF field E_g. Considering the second-order beat frequency interaction between the LF field and the HF Lagmuir wave, one of us had derived the equations of the HF field and of the slowly varying electron distribution function by use of the Vlasov-Poisson equation [20]. The HF Langmuir field obtained from the above ideal is completely consistent with that obtained from the Zakharov equations or the cubically nonlinear Schrödinger equation. The LF oscillation electron distribution function consisting of δF and F_0 can be approximately expressed into the following form [20]:

$$F(X,V,0)=F_0(V)\left[1+\frac{|E(X)|^2}{8\pi n_e k_B T}(V^2-2)\right], \tag{13}$$

where V is dimensionless velocity and

$$F_0(V)=\frac{1}{\sqrt{2\pi}}e^{-V^2/2} \tag{14}$$

is a Maxwellian distribution. In simulation, we have replaced electric fields $E(X)$ by the Fourier modes structure.

It is clear that the distribution function remains positive as $0<E_0^2/8\pi n_e k_B T<0.5$. From Fig. 7, we observe that the initial distribution function $F(X,V,0)$ at $X=0$ has a symmetrical double-peak structure, which results from particles interacting with low-frequency fields and ponderomotive potential [20]. In addition, this structure would be destroyed with the particle trajectory stochasticity. He [21] had shown that spatially inhomogeneity plays a dominant role in a certain range of velocity for clump formation. These particles would run out of the soliton and carry the interaction information between particles and waves, i.e., cause a rearrangement of the average distribution function.

In the study of clumps, usually people try to discuss the correlation function through a renormalization of the two-point correlation from the Vlasov equation [9–11] or using a particle simulation technique [12,13]. For our inhomogeneous plasmas; however, the renormalized turbulent technique is no longer valid. Hence, we consider the two-point correlation function that exhibits the mi-

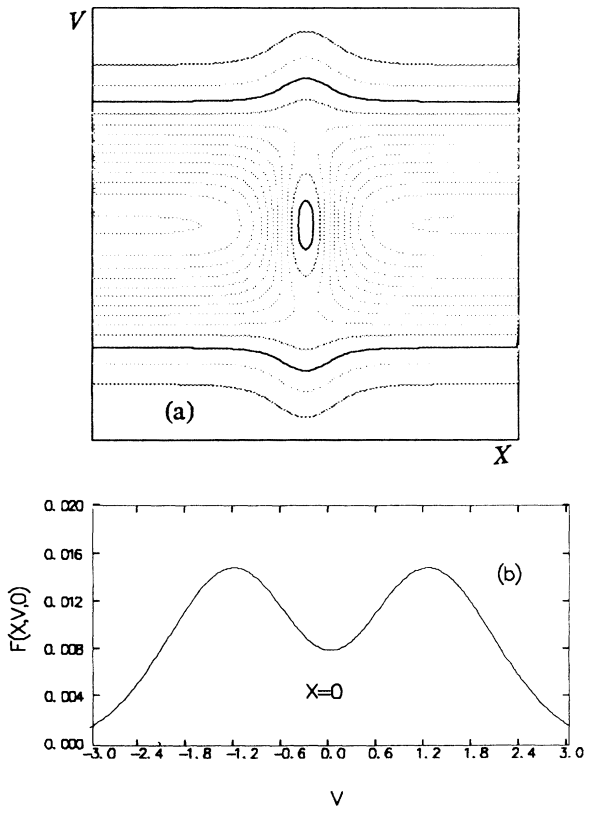

FIG. 7. (a) Contours of the initial electron distribution function $F(X,V,0)$. (b) Plot of the initial electron distribution function $F(X,V,0)$ with $X=0$.

croscale correlation behavior by the particle simulation technique. In simulation, we assume that the initial electrons are localized in a soliton envelope, i.e., $X_i \in [-16,16]$, $V_i \in [-3,3]$. The initial size of each cell is taken as $(\Delta X, \Delta V)=(0.1,0.1)$.

The particles in the ith cell can be calculated by integrating

$$N_i(t=0)=n_0 \int_{X_1-\Delta X/2}^{X_i+\Delta X/2} \int_{V_i-\Delta V/2}^{V_i+\Delta V/2} F(X_i', V_i', 0) dX_i' dV_i' \ . \tag{15}$$

To measure the correlation function $\langle \delta f(X_1, V_1, t) \delta f(X_2, V_2, t) \rangle$ for small $r^0=X_1-X_2$ and $u^0=V_1-V_2$, we define the fluctuation δf of the distribution function as $\delta f_i = N_i - \langle N_i \rangle / \langle N_i \rangle$. The simulated correlation function can be expressed as

$$\langle \delta f(1) \delta f(2) \rangle = \frac{1}{m} \sum_m [\delta f(1) \delta f(2)]_i \ , \tag{16}$$

where m represents the experimental ensemble average times. The whole calculation is repeated 50 times. From the numerical results given in the above section, we have known that the microscale correlation time (or so-called clump lifetime) is finite. Here, we measure the correlation function at $t=60$. The particles at $t=60$ can be obtained by way of tracing the orbit of each particle lying in the initial cells. In addition, we simultaneously calculate the coherent correlation function $\langle \delta f^{(c)}(1) \delta f^{(c)}(2) \rangle$, which is obtained by use of the method of unperturbed particle orbits, and define $C(1,2)=\langle \delta f(1) \delta f(2) \rangle - \langle \delta f^{(c)}(1) \delta f^{(c)}(2) \rangle$ as the correlation function of clumps.

Figures 8 and 9 are the simulated numerical results. Comparing the correlation function $\langle \delta f(1) \delta f(2) \rangle$ with $\langle \delta f^{(c)}(1) \delta f^{(c)}(2) \rangle$, we observe that the peak behavior of $\langle \delta f(1) \delta f(2) \rangle$ only occurs for very small r^0 and u^0. As far as the coherent part $\langle \delta f^{(c)}(1) \delta f^{(c)}(2) \rangle$ is concerned, it is nearly a smooth function for r^0 and u^0; that is, $\langle \delta f^{(c)}(1) \delta f^{(c)}(2) \rangle$ does not have peak phenomena as r^0 and u^0 become smaller and smaller. Obviously, the whole correlation is much greater than that for coherent parts with sufficiently small r^0 and u^0. With r^0 and u^0 increasing, $\langle \delta f(1) \delta f(2) \rangle$ tends to $\langle \delta f^{(c)}(1) \delta f^{(c)}(2) \rangle$.

As to the relative diffusion [see Figs. 3(b) and 4(b)], we know that the correlation length of neighboring particles is less than λ_D. The same conclusion can be given in terms of the current simulation results (see Fig. 8). In addition, we find in simulation that the peak behavior of the correlation function depends on the barycentric positions in phase space, i.e., is associated with the diffusion in ve-

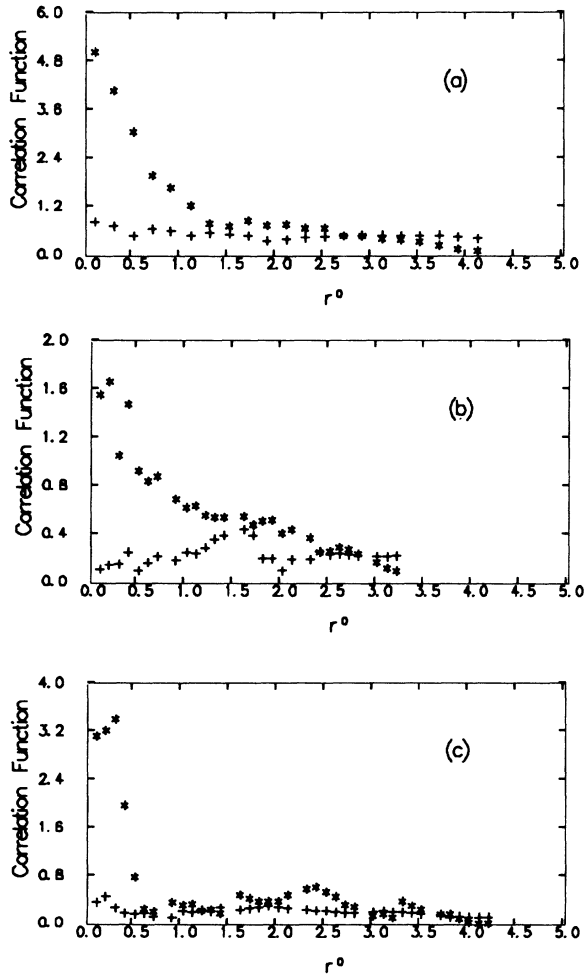

FIG. 8. Two-point correlation function calculated from the particle simulation vs r^0 with $u^0=0.4$. The asterisk represents the correlation function $\langle \delta f(1) \delta f(2) \rangle$. The plus shows the coherent part $\langle \delta f^{(c)}(1) \delta f^{(c)}(2) \rangle$. (a) $X_1=100.0$, $V_1=2.25$; (b) $X_1=100.0$, $V_1=1.25$; (c) $X_1=125.0$, $V_1=2.0$.

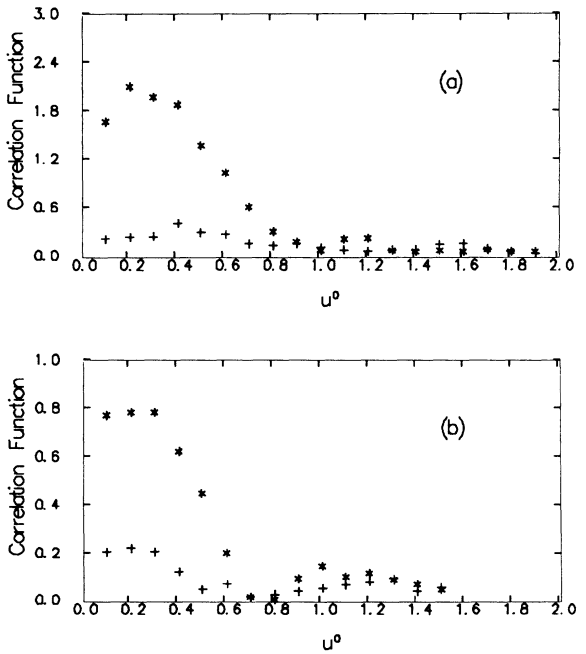

FIG. 9. Two-point correlation function calculated from the particle simulation vs u^0 with $r^0=0.4$, the symbols are as indicated in Fig. 8. (a) $X_1=125.0$, $V_1=2.0$; (b) $X_1=100.0$, $V_1=1.5$.

locity space as well as that in configuration space. Although the theoretical work for discussing the two-point correlation function of the inhomogeneous system has not been obtained as yet, we can conclude from current numerical results that the equation of the two-point correlation function would also contain terms to describe the relative diffusion behavior in configuration space, which is different from that discussed by Dupree and others [8–11] for spatially homogeneous plasmas. In their equation, only the relative velocity diffusion coefficient is exhibited.

VI. CONCLUSIONS

A numerical simulation of the dynamic properties for electrons in localized coherent Langmuir fields has been given. It is shown that these coherent wave packets lead to particle stochastic diffusion. The coexistence of irregular motions, trapped orbits, secondary resonances, and the KAM surfaces can be illustrated by the Poincaré mapping and the absolute diffusion coefficient. In plasma turbulence, the random fields derive particle trajectory stochasticity. The mixing of "fluids" of different densities would lead to the formation of microscale random phase-space granulations or clumps. These microscale structures may be an important mechanism in anomalous transport [7].

For our dynamic system, on the other hand, the intrinsic stochasticity is due to the phase velocities of the modes satisfying the overlapping criterion. Liouville's theorem also preserves the different densities from interpenetrations. When neighboring particles lie in the sufficiently small cell, however, they may be subject to the same force and behave like a single large discrete particle or macroparticle during a finite time. The basic properties for such a "macroparticle" can be described by the relative diffusion of neighboring particles and the two-point correlation function. From the numerical results, we find that the microscale phase-space granulations for electrons can also occur due to the interaction of the coherent Langmuir wave packets. The time evolutions of relative quantities further show that the lifetime of the microscale correlation is finite. In particular, the strong correlation behavior for sufficiently small r^0 and u^0 has been exhibited by our particle simulation.

Finally, we should mention the main difference between our results and those obtained by some authors. In the work of Rozmus and co-workers [4,5], they only discussed the one-particle diffusion. Although the resonance structures can well be explained in terms of their theoretical and numerical work, the dynamics behaviors of neighboring particles has not been analyzed. In our previous work [1], we analytically gave the relative diffusion coefficient and lifetime of the microscale correlation by considering the Wiener ensemble average [22], but the time evolution of relative quantities and the two-point correlation function were not discussed. In addition, Dupree and co-workers [7–13] were only involved with the spatial homogeneous or weak inhomogeneous plasmas. Their theoretical or numerical work is of great significance in the study of plasma turbulence and the mechanism of anomalous transport. In our current work, we systematically investigate the dynamics behaviors of one particle and two particles, while, on the other hand, the spatial inhomogeneous plasmas are dealt with. It is also worth noting that the interaction of particles with coherent wave packets is the central problem of plasma turbulence and laser plasmas, etc. We expect that our analysis, therefore, can prove to be useful in understanding the basically physical picture.

ACKNOWLEDGMENTS

We would like to acknowledge useful discussions with Professor S. G. Chen. This work has been supported by the National Natural Science Foundation of China, Grant No. 1880109.

[1] Shao-ping Zhu and X. T. He, Phys. Rev. A **43**, 1988 (1991).
[2] V. Fuchs, V. Krapchev, A. Ram, and A. Bers, Physica **14D** 141 (1985).
[3] M. Colunga, J. F. Luciani, and P. Mora, Phys. Fluids **29**, 3407 (1986).
[4] W. Rozmus, J. C. Samson, and A. A. Offenberger, Phys. Lett. A **126**, 263 (1988).
[5] W. Rozmus and J. C. Samson, Phys. Fluids **31**, 2904 (1988).
[6] X. T. He and Y. Tan, Bull. Am. Phys. Soc. **34**, 7162 (1988).
[7] T. H. Dupree, Phys. Rev. Lett. **25**, 789 (1970).
[8] T. H. Dupree, Phys. Fluids **15**, 334 (1972).
[9] T. H. Dupree, Phys. Fluids **18**, 1167 (1975).
[10] T. Boutros-Ghali and T. H. Dupree, Phys. Fluids **24**, 1839 (1981).
[11] R. Balescu and J. M. Misguich, in *Statistical Physics and Chaos in Fusion Plasmas,* edited by C. W. Horton, Jr. and L. E. Reichl (Wiley, New York, 1984), p. 295.
[12] B. H. Hui and T. H. Dupree, Phys. Fluids **18**, 235 (1975).
[13] H. R. Bermain, D. J. Tetrealt, and T. H. Dupree, Phys. Fluids **26**, 2437 (1983).
[14] D. R. Nicholson, *Introduction to Plasma Theory* (Wiley, New York, 1983).
[15] G. M. Zaslavsky, *Chaos in Dynamic Systems* (Harwood, London, 1985).
[16] R. Z. Segdeev, D. A. Usikov, and G. M. Zaslavsky, *Nonlinear Physics* (Harwood, London, 1988).
[17] A. J. Lichtenberg and M. A. Lieberman, *Regular and Stochastic Motion* (Springer-Verlag, New York, 1983).
[18] J. M. Misguich and R. Balescu, Plasma. Phys. **25**, 289 (1982).
[19] M. Pettini, A. Vulpiani, J. H. Misguich, M. D. Leener, J. Orban, and R. Balescu, Phys. Rev. A **38**, 344 (1988).
[20] X. T. He, Chin. Phys. **8**, 9 (1988).
[21] H. T. He (unpublished).
[22] A. Salat, Phys. Fluids **31**, 1499 (1988).

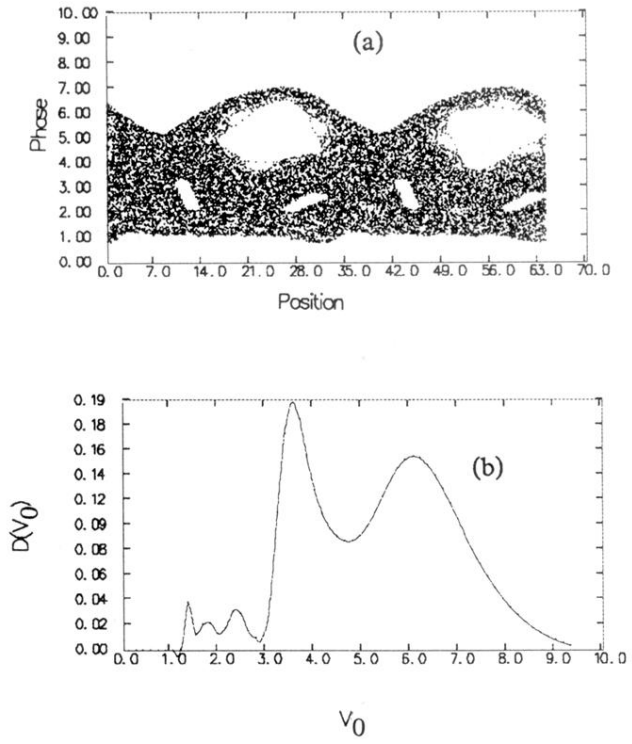

FIG. 2. (a) Poincaré surface of the section plot, based on numerical solutions to the equations of motions (2). (b) Absolute diffusion coefficient.